CORE
Metadata, citation and similar papers at core.ac.uk
Provided by Apollo

MNRAS **464,** L1–L5 (2017)
Advance Access publication 2016 August 30
doi:10.1093/mnrasl/slw170

Do sound waves transport the AGN energy in the Perseus cluster?

A. C. Fabian,[1]★ S. A. Walker,[1] H. R. Russell,[1] C. Pinto,[1] J. S. Sanders[2] and C. S. Reynolds[3]

[1]*Institute of Astronomy, Madingley Road, Cambridge CB3 0HA, UK*
[2]*Max-Planck-Institut für Extraterrestrische Physik, Giessenbackstrasse 1, D-85748 Garching, Germany*
[3]*Department of Astronomy, University of Maryland, College Park, MD 20712-2421, USA*

Accepted 2016 August 24. Received 2016 August 22; in original form 2016 July 28

ABSTRACT

The level of random motions in the intracluster gas lying between 20 and 60 kpc radius in the core of the Perseus cluster has been measured by the Hitomi Soft X-ray Spectrometer (SXS) at $164 \pm 10\,\mathrm{km\,s^{-1}}$. The maximum energy density in turbulent motions on that scale is therefore low. If dissipated as heat, the turbulent energy will be radiated away in less than 80 Myr and cannot spread across the core. A higher velocity is needed to prevent a cooling collapse. Gravity waves are shown to travel too slowly in a radial direction. Here we investigate propagation of energy by sound waves. The energy travels at $\sim 1000\,\mathrm{km\,s^{-1}}$ and can cross the core in a cooling time. We show that the displacement velocity amplitude of the gas required to carry the power is consistent with the Hitomi result and that the inferred density and temperature variations are consistent with *Chandra* observations.

Key words: galaxies: clusters: intracluster medium – X-rays: galaxies.

1 INTRODUCTION

The Soft X-ray Spectrometer (SXS) on the Hitomi satellite has recently measured the level of gas motions in the X-ray bright intracluster medium (ICM) in the core of the Perseus cluster (Fig. 1) to an unprecedented precision of $10\,\mathrm{km\,s^{-1}}$ (Hitomi collaboration 2016). Small-scale motions (< 10 kpc) in a region 20–60 kpc from the central active galactic nucleus (AGN) are $164 \pm 10\,\mathrm{km\,s^{-1}}$; larger scale shear across that region is also low, i.e. $\sim 150 \pm 70\,\mathrm{km\,s^{-1}}$. The energy density of turbulent motions is at most 4 per cent of the thermal energy density of the hot intracluster gas.

In the absence of a heat source, the hot gas in this region would cool radiatively, due to the emission of X-rays, on a time-scale of 1−2 Gyr forming a massive cooling flow of several hundred $\mathrm{M_\odot\,yr^{-1}}$ (see e.g. Fabian 2012). Although the temperature of the hot gas does drop towards the centre, little gas is seen below 3 keV, ruling out such a cooling flow. If all the energy in random motions is ascribed to turbulence which is then dissipated as heat, then it will be used up in 4 per cent of the cooling time: it needs to be replenished on the same time-scale, which is about 8×10^7 yr. However, if the velocity at which energy flows is limited to $164\,\mathrm{km\,s^{-1}}$, then the energy can only travel 13 kpc in that time-scale, before being lost as radiation. Energy needs to be transported from the energy source – the AGN – at a much higher velocity of at least $700\,\mathrm{km\,s^{-1}}$, close to the speed of sound in the region ($\sim 1000\,\mathrm{km\,s^{-1}}$). One energy transport mechanism that can do this is sound waves. The matter does not flow but the energy does. Here we explore further the case for the importance of sound waves in the Perseus and other cool core clusters. The observed velocity dispersion is consistent with that required to transport the energy required for heating the cluster core.

Many studies of cool-core clusters (Bîrzan et al. 2004, 2012; Dunn & Fabian 2006, Dunn & Fabian 2008; Fabian 2012; McNamara & Nulsen 2012) have shown that the bubbles produced by jets from the central black hole represent a considerable energy flow which is capable of balancing radiative cooling (e.g. Churazov et al. 2002). What has remained unclear is the means by which the energy from the bubbles is transported throughout the core and distributed in a roughly isotropic manner. Ripples with a wavelength ∼15 kpc were seen in the first deep *Chandra* images of the Perseus cluster and interpreted as sound waves (Fabian et al. 2003). Their amplitude was consistent with the required energy flux. Issues of dissipation were explored by Fabian et al. (2005). Sound wave propagation and dissipation in intracluster gas were simulated by Ruszkowski, Brüggen & Begelman (2004a,b), Brüggen, Ruszkowski & Hallman (2005), Sijacki & Springel (2006), Sternberg & Soker (2009) and have been further discussed by Mathews, Faltenbacher & Brighenti (2006) and Heinz & Churazov (2005).

The ripples became clearer in yet deeper *Chandra* observations (Fabian et al. 2006; Sanders & Fabian 2007). The expected temperature changes associated with sound waves were at the limit of detectability in these observations and were not seen. Later work on surface brightness fluctuations found in these observations were interpreted by Zhuravleva et al. (2014) as due to turbulence. This was then extended to cover two X-ray colour bands, making the work sensitive to temperature fluctuations and with a goal of

★ E-mail: acf@ast.cam.ac.uk

© 2016 The Authors
Published by Oxford University Press on behalf of the Royal Astronomical Society

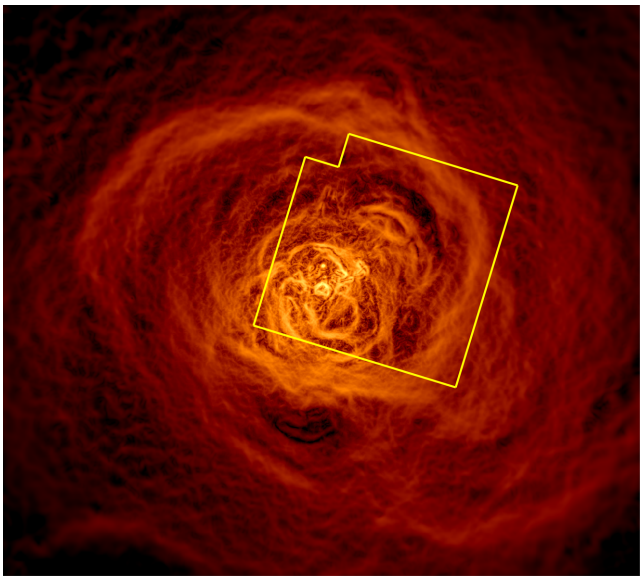

Figure 1. The core of the Perseus cluster filtered with an edge-detection algorithm (Sanders et al. 2016b) and overlaid with the field of view of the Hitomi SXS (3 arcmin × 3 arcmin, or about 60 kpc × 60 kpc).

testing the equation of state of the fluctuations. The ripples were not, however, bright enough to be separately analysed (see Zhuravleva et al. 2016 and Section 3). A similar analysis has been made of the ICM around M87 by Arévalo et al. (2016).

2 THE GENERATION AND PROPAGATION OF TURBULENT MOTIONS

Reynolds, Balbus & Schekochihin (2015) have examined the generation of subsonic turbulence through 3D hydrodynamical simulation of AGN-like events. Gravity waves (g modes) are launched by these events into the ICM and decay to volume-filling turbulence. They find, however, that the process is very inefficient with less than 1 per cent of the energy injected by the AGN activity ending up as turbulence in the ICM. Yang & Reynolds (2016) have then used further hydrodynamical simulations to explore momentum-driven jet feedback, confirming that the level of turbulent heating is low, accounting for only about 1 per cent of the energy. Turbulence is not necessarily an essential ingredient of cluster AGN feedback.

Still, it is possible that processes not captured by these simple hydrodynamic models might lead to a significantly stronger AGN driving of the g modes (see section 6 of Reynolds et al. 2015) and so it is interesting to examine the subsequent propagation speed of the g modes. Working within a local/WKB approximation, the dispersion relation for a particular g mode with (angular) frequency ω and wavevector $\boldsymbol{k}$ is $\omega^2 = N^2 k_{\rm h}^2/|\boldsymbol{k}|^2$, where $k_{\rm h}$ is the horizontal component of the wavevector and N is the Brunt–Väisälä frequency given by

$$N^2 = -\frac{c_{\rm s}^2}{\gamma}\frac{\partial(\ln\rho)}{\partial z}\frac{\partial(\ln P\rho^{-\gamma})}{\partial z}, \qquad (1)$$

($c_{\rm s}$ is the adiabatic sound speed, ρ is density, P is pressure, and γ is the adiabatic index which we take to be $\gamma = 5/3$). Energy propagates at the group velocity, $\boldsymbol{v}_{\rm g} = \nabla_k\omega$, and so the outwards/radial speed of propagation is

$$v_{\rm g,r} = \frac{\partial\omega}{\partial k_{\rm r}} = \sin\theta\cos^2\theta\frac{N}{k_{\rm r}}. \qquad (2)$$

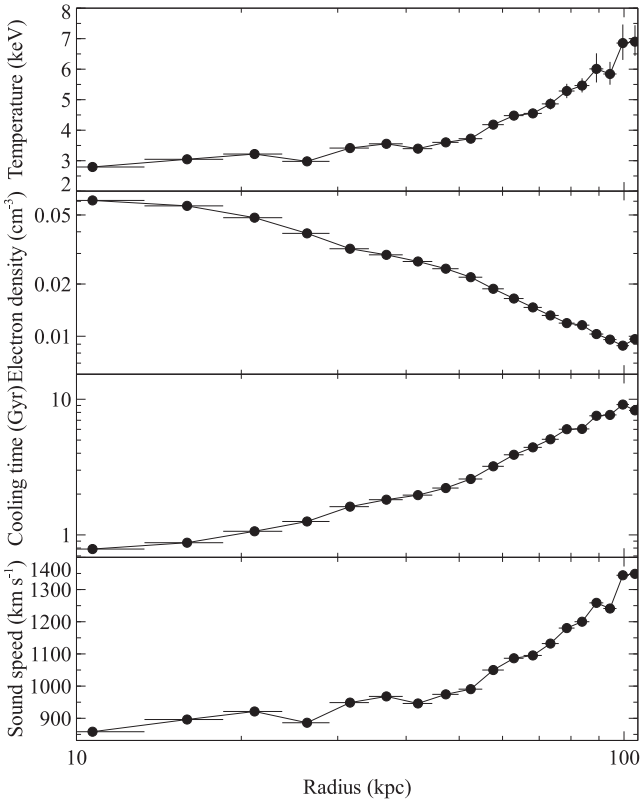

Figure 2. Profiles of the intracluster temperature, density, radiative cooling time and sound speed in the Perseus cluster.

Here, θ is the angle that the propagation direction makes with the outwards pointing direction and $k_{\rm r}$ is the radial component of the wavevector. Since $|\sin\theta\cos^2\theta| < 2/3\sqrt{3} \approx 0.38$, we see that $v_{\rm g,r} < 0.38(N/2\pi)(2\pi/k_{\rm r})$ – this has the simple interpretation that, with each buoyant cycle, the g mode propagates upwards by (at most) half of a radial wavelength $\lambda_{\rm r} = 2\pi/k_{\rm r}$.

If H_ρ and $H_{\rm S}$ are the density and entropy scaleheights, equation (1) becomes $N = c_{\rm s}/\sqrt{\gamma H_\rho H_{\rm S}}$ and we find that

$$v_{{\rm g},z} < 0.047 c_{\rm s}\frac{\lambda_{\rm r}}{\sqrt{H_\rho H_{\rm S}}}, \qquad (3)$$

so we immediately see that the g modes propagate very subsonically, provided that $\lambda_{\rm r} < H_\rho, H_{\rm S}$ (note that if this condition were violated, the local approximation used here would break down). Measurements of the temperature and density profiles in Perseus (Fig. 2) imply scaleheights of $H_\rho, H_{\rm S} \sim 30$–$50$ kpc which, when compared with the ∼15 kpc radial wavelength of the observed ripples, yields radial propagation speeds for the g modes of $v_{{\rm g},z} < 0.02 c_{\rm s} \approx 20$–$30\,{\rm km\,s^{-1}}$. Even taking the maximum wavelength possible ($\lambda_{\rm r} \sim H_\rho$) yields $v_{{\rm g},z} < 0.05 c_{\rm s} \approx 50$–$70\,{\rm km\,s^{-1}}$. These g-mode propagation velocities are at least an order of magnitude too small to replenish the decaying turbulence, if the turbulence is indeed responsible for offsetting the radiative cooling.

The sharp high-energy edge to the Fe Heα resonance line observed from the Perseus cluster by the Hitomi SXS leaves no room for any significant component with larger velocity motions.

3 SOUND PROPAGATION

The energy in a sound wave is carried at the speed of sound, as the particles oscillate about their mean position at a much lower

(displacement) velocity. If the energy density due to random motions is $\frac{1}{2}\rho v_r^2$, where v_r is the gas velocity then the maximum rate at which energy flows from a central source is

$$\mathcal{P}_v = 2\pi r^2 \rho v_r^3. \quad (4)$$

The energy flux due to sound waves which have a displacement velocity amplitude v_s is

$$\mathcal{P}_s = 4\pi r^2 c_s \rho v_s^2. \quad (5)$$

Sound waves can therefore transport $2c_s/v_r$ times more power than random motions alone, for a given measured velocity. This is over an order of magnitude increase in the case of the Perseus cluster considered here, where $c_s \sim 1000\,\mathrm{km\,s^{-1}}$ and $v_r \sim 164\,\mathrm{km\,s^{-1}}$.

In order to determine the displacement velocity from the observed broadening of emission lines, we need to correct for projection effects. We achieve that by simulating a cluster of as many cubic cells of size matching the SXS 10 kpc pixels, each containing gas of the appropriate density and temperature to match observed profiles (Fig. 2). Assigning a radial velocity to the gas in each cell according to a radial sine wave enables us to assemble the emission-weighted line profile as a function of projected radius (Fig. 3: the intrinsic profile is shown in the upper panel and the profile which would be observed, after convolution with the instrumental and thermal broadening, is shown in the lower panel). The sharp peak is due to the brightest gas along any line of sight lying in the plane of the sky where the apparent radial displacement velocity of the gas is zero. We measure one standard deviation of that profile (68 per cent of the total emission from the line centre) and use that value. It varies with radius and is between about one-third to one-half of the amplitude of the true displacement velocity. This yields another factor of at least 4 in favour of sound wave propagation. (The $200\,\mathrm{km\,s^{-1}}$ used for Fig. 3 is a fiducial value.)

If all the measured dispersion is attributed to radial sound waves, then their intrinsic velocity amplitude would be about $300\,\mathrm{km\,s^{-1}}$. It is possible, of course, that the observed dispersion is a combination of sound waves of lesser amplitude with other random motions and turbulence.

Future microcalorimeters with higher spectral resolution, such as the planned X-ray Integral Field Unit (Barret et al. 2016) on ESA's Athena X-ray Observatory may be able to measure the non-Gaussian nature of the perturbations caused by sound waves.

We note that the recent simulations of Yang & Reynolds (2016) provide strong support for the idea that sound waves are a major contributor to the ICM velocities. They use a Helmholtz decomposition to separate compressible motions (sound waves and shocks) from incompressible motions (turbulence and large-scale circulation) in their simulations of a Perseus-like cluster with self-regulation by a jetted AGN. Throughout most of the volume of the cluster core (i.e. the region away from the 'jet cones') at a typical snapshot in time, the compressible motions dominate with a magnitude $v_s \sim 150\,\mathrm{km\,s^{-1}}$; turbulent velocities are somewhat less ($v_{\mathrm{turb}} \sim 100\,\mathrm{km\,s^{-1}}$) with bulk flow and circulatory motions being smaller yet (Karen Yang, private communication). Since the Yang & Reynolds simulations adopt an ideal hydrodynamic framework, there are no mechanisms that can efficiently dissipate the sound waves, and thus the heating actually occurs via bubble mixing and weak shocks in the jet cone, with a gentle circulation that cycles a large part of the ICM through this region on Gyr time-scales. The expectation is that, given the inclusion of a suitable dissipation mechanism, sound wave heating will be important in future developments of these models.

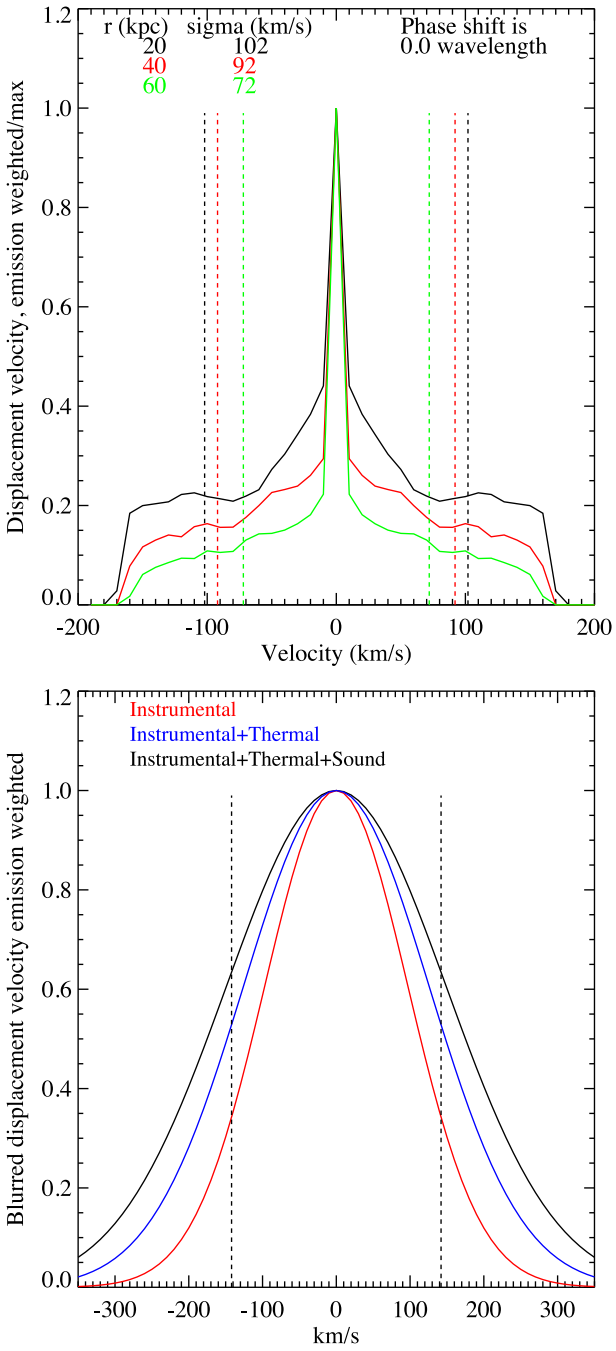

Figure 3. Top: simulated line profiles due to the effect of the displacement velocity of sound waves in the ICM of the Perseus cluster. The profiles shown are for three different lines of sight passing at increasing distances from the core, spanning the range covered by the Hitomi observation (20, 40 and 60 kpc), and using the same pixel size as the Hitomi SXS. The line-of-sight component of the displacement velocity was integrated through the cluster along these sightlines, weighted by the emission measure of the gas. The corresponding coloured dashed vertical lines show the width containing 68 per cent of the line strength. There is only a small change if the phase of the sound waves is shifted by half a wavelength. Bottom: appearance of the line profile expected at 40 kpc offset, after convolution with both instrumental and thermal broadening.

4 TEMPERATURE FLUCTUATIONS IN SOUND WAVES

Adiabatic sound waves are accompanied by temperature fluctuations

$$\frac{\Delta T}{T} = \frac{2}{3}\frac{\Delta n}{n} \approx \frac{1}{3}\frac{\Delta I}{I}, \tag{6}$$

where I is the soft X-ray surface emissivity.

Projection effects reduce the apparent amplitude of sound waves as observed in X-rays in ICM (Graham, Fabian & Sanders 2008), such that waves with a density amplitude of 5 per cent, which leads to an emissivity fluctuation of about 10 per cent (ie $\propto n^2$), can appear as a surface brightness fluctuation of only 3–5 per cent. (The observed fluctuations are about ±3 per cent at radii of 20–60 kpc in the Perseus cluster; Sanders & Fabian 2007.)

Projection also affects the amplitude of the accompanying temperature fluctuations: all lines of sight contain variations, but some have more than others. In order to estimate these affects, we have used the same simulation as mentioned above for the velocity; only now we calculate the integrated spectrum along the line of sight. (The pixels and response files now match those of *Chandra*.) Such spectra are then converted to hardness ratios (Fig. 4). We employ the bands 0.5−4 keV and 4−8 keV as used by Zhuravleva et al. (2016); the harder band is much more temperature dependent than the softer one. It is clear that it is very difficult to measure periodic variations in the hardness ratio unless the exposure is significantly longer that the current one. We have also measured from the simulation the hardness ratio of the relative fluctuations in each band, which Zhuravleva et al. (2016) and Churazov et al. (2016) show is sensitive to the effective equation of state of the ICM. The resulting value is 1 ± 0.2 which is consistent with isolated isothermal perturbations. The adiabatic perturbations used in the simulation appear isothermal due to the large effect of projection.

5 GENERATION AND DISSIPATION OF SOUND

We are here considering the situation where the bubbling energy of the AGN is converted into mechanical motions in the gas which is transported throughout the cluster core and dissipated there. The above estimates and the observed limiting level on turbulent velocity preclude turbulence as the sole basis of the mechanical motions which heat the whole cluster core. Sound waves remain possible as the transport mechanism because they transport energy much faster.

Sound waves can be generated during the inflation stage of the bubbles, particularly if the jets are unsteady. Malzac (2014) has successfully modelled the jets of some X-ray binaries by relating the spectrum of variations in the accretion flow to the acceleration of matter in the jet. The AGN at the centre of the Perseus cluster, in the galaxy NGC1275, is known to vary by over a factor of 30 over the past four decades (Fabian et al. 2015 and references therein). It may plausibly vary by even larger factors and many times over the much longer time taken to form the bubbles.

The bubbles may themselves oscillate especially as they detach and rise. The natural frequency of a bubble, the Minnaert frequency

$$f_{\rm M} = \frac{1}{2\pi r_{\rm b}}\left(\frac{3\gamma p_{\rm A}}{\rho}\right)^{1/2}. \tag{7}$$

This leads a wavelength of about $4r_{\rm b}$, where $r_{\rm b}$ is the bubble radius, $p_{\rm A}$ is the ambient pressure and ρ the density of the surrounding medium. Such a large wavelength (∼30 kpc) is probably too large to be relevant.

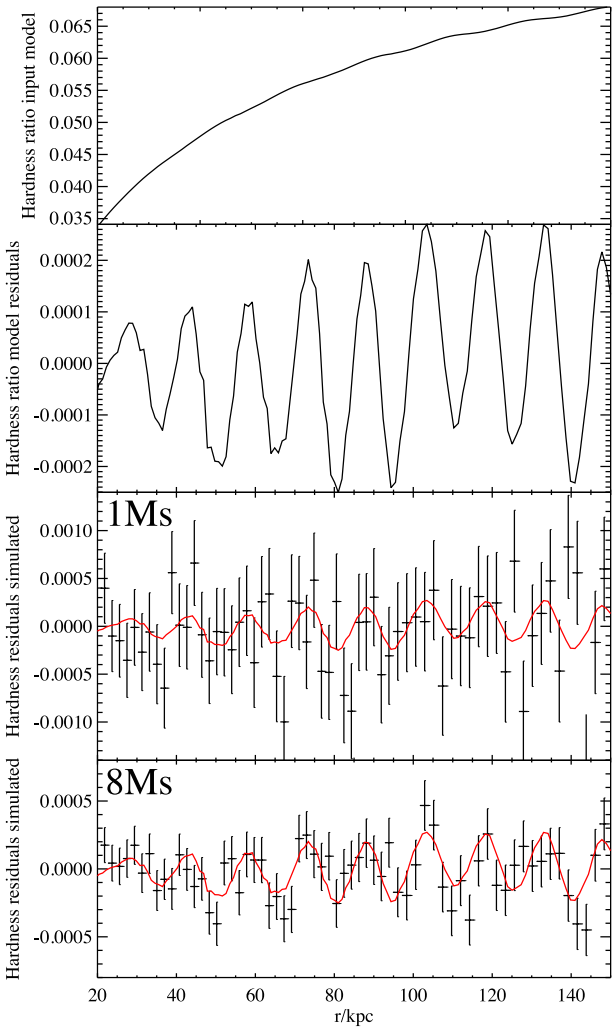

Figure 4. Simulated hardness ratio profiles, using 4.0–8.0 keV for the hard band and 0.5–4.0 keV for the soft band. Top: the input model for the hardness profile, taking into account projection effects. Second: the residuals in the input hardness ratio model due to the input sound waves. Third: hardness ratio residuals in a 1 Ms simulated observation, compared to the input model (red). Fourth: hardness ratio residuals in an 8 Ms simulated observation.

It is also likely that the $5 \times 10^{10}\,{\rm M}_\odot$ of cold molecular gas in the core of the cluster (Salomé et al. 2011) oscillates in response to the bubbling process and so generates further sound waves.

The power of the sound,

$$\begin{aligned}\mathcal{P}_{\rm s} &= 4\pi r^2 c_{\rm s}\rho v_{\rm s}^2 \\ &= 2.9\times10^{44}\left(\frac{r}{40\,{\rm kpc}}\right)^2\left(\frac{v}{200\,{\rm km\,s^{-1}}}\right)^2\,{\rm erg\,s^{-1}} \\ &= 4\pi r^2\frac{\delta P^2}{\rho c_{\rm s}},\end{aligned} \tag{8}$$

where P is the gas pressure and δP is the pressure change associated with the sound wave. Note that

$$\frac{\delta P}{P} = \frac{v}{c_{\rm s}}. \tag{9}$$

The power scaling is close to that required to compensate for radiative energy losses in the cluster core (see fig. 5 of Sanders & Fabian 2007). The exact level required depends on the length of time since the present configuration of intracluster gas has lasted. Given

the level of sloshing seen in the cluster, this could be 4–5 Gyr, which agrees with the required power estimates of $2.5-5 \times 10^{44}$ erg s^{-1} at 40 kpc radius. The power required at 10 kpc is $6-8 \times 10^{44}$ erg s^{-1}, with the difference having been dissipated at radii between 10 and 40 kpc.

The required dissipation length is 50–70 kpc. How the energy might be dissipated by sound waves has been considered by Ruszkowski et al. (2004a) and Fabian et al. (2005) and remains an open question. Simple hydrodynamic viscosity and conduction may be insufficient. Tangled magnetic fields may give a bulk viscosity as sound wave propagation changes the field configuration in a non-reversible manner.

Sound waves will refract and reflect from density changes and discontinuities, including cold fronts, meaning that the situation will not be simple but, at radii of a few wavelengths, approach that of a noisy room.

Weak shocks and possible sound waves have previously been reported from M87 (Forman et al. 2007), the Centaurus cluster (Sanders et al. 2009, Sanders et al. 2016a) and A2052 (Blanton et al. 2011). Difficulties in detecting sound waves, in part due to projection effects, have been explored by Graham et al. (2008) and reveal that most current exposures are far too short. Walker, Sanders & Fabian (2016) have shown that edge-detection (Gaussian gradient magnitude, GGM) techniques can increase the contrast of sound waves in X-ray images. That work and the GGM images of Sanders et al. (2016b; see also Fig. 1 here) show that elongated, azimuthal structures are relatively common in cool core clusters.

The Hitomi SXS result demonstrates that cluster AGN feedback cannot just involve turbulence. We show here that sound waves, first observed with the necessary level of surface brightness fluctuations in 2003, have a velocity amplitude consistent with both the Hitomi spectrum and the propagation of AGN power through the cool core of the Perseus cluster. We anticipate that generation of powerful sound waves by AGN feedback is present in all cool core groups and clusters and is a major part of the feedback loop.

ACKNOWLEDGEMENTS

ACF, CP, CSR and HRR thank the Hitomi collaboration for the opportunity to participate in the analysis of the SXS data. ACF, CP, HRR and SAW acknowledge support from ERC Advanced Grant FEEDBACK, 340442.

REFERENCES

Arévalo P., Churazov E., Zhuravleva I., Forman W. R., Jones C., 2016, ApJ, 818:14
Barret D. et al., 2016, SPIE Conf. Proc., in press, preprint (arXiv:1608.08105)
Bîrzan L., Rafferty D. A., McNamara B. R., Wise M. W., Nulsen P. E. J., 2004, ApJ, 607, 800
Bîrzan L., Rafferty D. A., Nulsen P. E. J., McNamara B. R., Rottgering H. J. A., Wise M. W., Mittal R., 2012, MNRAS, 427, 3468
Blanton E., Randall S. W., Clarke T. E., Sarazin C. L., McNamara B. R., Douglass E. M., McDonald M., 2011, ApJ, 737, 99
Brüggen M., Ruszkowski M., Hallman E., 2005, ApJ, 630, 740
Churazov E., Arevalo P., Forman W., Jones C., Schekochihin A., Vikhlinin A., Zhuravleva I., 2016, MNRAS, 463, 1057
Churazov E., Sunyaev R., Forman W., Böhringer H., 2002, MNRAS, 332, 729
Dunn R. J. H., Fabian A. C., 2006, MNRAS, 373, 959
Dunn R. J. H., Fabian A. C., 2008, MNRAS 385, 757
Fabian A. C., 2012, ARA&A, 50, 455
Fabian A. C., Sanders J. S., Allen S. W., Crawford C. S., Iwasawa K., Johnstone R. M., Schmidt R. W., Taylor G. B., 2003, MNRAS, 344, L43
Fabian A. C., Reynolds C. S., Taylor G. B., Dunn R. J. H., 2005, MNRAS 363, 891
Fabian A. C., Sanders J. S., Taylor G. B., Allen S. W., Crawford C. S., Johnstone R. M., Iwasawa K., 2006, 366, 417
Fabian A. C., Walker S. A., Pinto C., Russell H. R., Edge A. C., 2015, MNRAS, 451, 3061
Forman W. et al., 2007, ApJ, 665, 1057
Graham J., Fabian A. C., Sanders J. S., 2008, MNRAS, 391, 1749
Heinz S., Churazov E., 2005, ApJ, 634, L141
Hitomi collaboration, 2016, Nature, 535, 117
McNamara B. R., Nulsen P. E. J., 2012, New J. Phys., 14, 5
Malzac J., 2014, MNRAS, 443, 299
Mathews W. G., Faltenbacher A., Brighenti F., 2006, ApJ, 638, 659
Reynolds C. S., Balbus S. A., Schekochihin A. A., 2015, ApJ, 815, 41
Ruszkowski M., Brüggen M., Begelman M. C., 2004a, ApJ, 611, 158
Ruszkowski M., Brüggen M., Begelman M. C., 2004b, ApJ, 615, 675
Salomé P., Combes F., Revaz Y., Downes D., Edge A. C., Fabian A. C., 2011, A&A, 531, 85
Sanders J. S., Fabian A. C., 2007, MNRAS, 381, 1381
Sanders J. S., Fabian A. C., 2009, MNRAS, 390, L93
Sanders J. S. et al., 2016a, MNRAS, 457, 82
Sanders J. S., Fabian A. C., Russell H. R., Walker S. A., Blundell K. M., 2016b, MNRAS, 460, 1898
Sijacki D., Springel V., 2006, MNRAS, 366, 397
Sternberg A., Soker N., 2009, MNRAS, 395, 228
Walker S. A., Sanders J. S., Fabian A. C., 2016, MNRAS, 461, 684
Yang H.-Y. K., Reynolds C. S., 2016, preprint (arXiv:1605.01725)
Zhuravleva I. et al., 2014, Nature, 515, 85
Zhuravleva I. et al., 2016, MNRAS, 458, 2902

This paper has been typeset from a TEX/LATEX file prepared by the author.